ELSEVIER

Journal of Chromatography A, 927 (2001) 1–17

JOURNAL OF CHROMATOGRAPHY A

www.elsevier.com/locate/chroma

Influence of the pH on the behavior of an imprinted polymeric stationary phase — supporting evidence for a binding site model

Yibai Chen[a,b], Marianna Kele[a,b,1], Igor Quiñones[a,b,2], Börje Sellergren[c], Georges Guiochon[a,b,*]

[a]*Department of Chemistry, The University of Tennessee, Knoxville, TN 37996-1600, USA*
[b]*Division of Chemical and Analytical Sciences, Oak Ridge National Laboratory, Oak Ridge, TN 37831, USA*
[c]*Department of Inorganic Chemistry and Analytical Chemistry, Johannes Gutenberg University, Mainz, Joh.–Joachim–Becherweg 24, D-55099 Mainz, Germany*

Received 22 December 2000; received in revised form 7 June 2001; accepted 7 June 2001

Abstract

The equilibrium isotherms of the two enantiomers of phenylalanine anilide (PA) were measured by conventional frontal analysis at three different pH on a thermally-treated imprinted stationary phase selective for the L enantiomer. The first of these pH (buffer pH=3.0, pH_{app}=4.0) is well below the apparent pK_a (6.4) of the two solutes, the second (buffer pH=5.8, pH_{app}=7.0) slightly below this pK_a, and the third (buffer pH=7.0, pH_{app}=8.3) well above it. The experimental data were fitted to several isotherm models. The best estimates of the parameters of these models are reported and discussed. The corresponding isotherms are compared with the experimental ones. The contributions of the enantioselective and nonselective interactions could be separated. The results obtained show that the saturation capacity is always smaller for D-PA than for L-PA, the template. The analytical separation is best at pH=3.0 because of a good separation factor (2.82) and short retention times. A good compromise between the resolution and the saturation capacity is obtained at pH=5.8, for which the best preparative separation is found. Both analytical and preparative results are poor at pH=7.0 because the separation factor is low (1.32). At this pH, the isotherm remains nearly linear in the whole concentration range accessible to measurements. The number of nonselective sites increases with increasing mobile phase pH slightly faster than the number of selective sites, suggesting different pK_a ranges for the two type of sites. Moreover, the binding energy and the homogeneity of the selective sites decreases with increasing pH. These results agree with a binding site model involving more than one carboxylic acid group, providing charge complementarity and hydrogen bond donors for binding of L-PA.

Keywords: pH effects; Imprinted polymeric stationary phase; Stationary phases, Lc; Enantiomer separation; Adsorption isotherms; Molecular imprinting; Binding site model; Phenylalanine anilide

1. Introduction

Molecular imprinting of cross-linked polymers is now widely used for the design of recognition materials for various chiral analytical and preparative separations [1–8]. The method consists in the poly-

*Corresponding author. University of Tennessee, Department of Chemistry, 552 Buehler Hall, Knoxville, TN 37996-1600, USA. Tel.: +1-865-974-0733; fax: +1-865-974-2667.
E-mail address: guiochon@utk.edu (G. Guiochon).
[1]Present address: Waters, Milford, MA, USA.
[2]Present address: Millipore, Bedford, MA, USA.

0021-9673/01/$ – see front matter
PII: S0021-9673(01)01019-6

merization of a functional monomer, mixed with a template, in the presence of a cross-linking agent. Removal of the template leaves an imprinted cavity in the polymer, providing a selective binding site for this template. In spite of the simplicity of this principle, the preparation of a separation material that performs well as a stationary phase for chromatography is not straightforward.

Numerous authors studied the preparation and performance of dedicated imprinted polymers for the separation of various mixtures, mostly of enantiomers [1–13]. Many of them investigated the molecular interactions between the template chiral molecule and the active site of these polymers [1,2,4,6,9]. An NMR study suggested the formation of a 1:2 complex between L-phenylalanine anilide (L-PA) and methacrylic acid, prior to polymerization, suggesting that there would be two binding groups per adsorption site (see Scheme 1) [10]. The mobile phase was a mixture of an organic solvent and an aqueous buffer. The pH of the buffer and its concentration in the mobile phase were shown to influence greatly the formation of labile complexes between the analyte and the polymer [8,11–13]. One common conclusion of these studies is that both hydrogen bonding and ion-exchange contribute to the molecular interactions between analyte and functional groups of the polymers. One study showed that the discriminating ability of the polymer was lost when the pH of the mobile phase exceeded the apparent pK_a of the polymer [8]. Another study showed that an electrostatic retention model could account for the retention of phenylalanine anilide when the pH of the mobile phase was varied between 2 and 9 [11]. Different results were obtained for more weakly basic templates [13]. A frontal and zonal chromatographic study of theophylline suggested that hydrogen bonding is the dominating interaction in that case, while ionic interactions appeared to be rather insignificant [9,13].

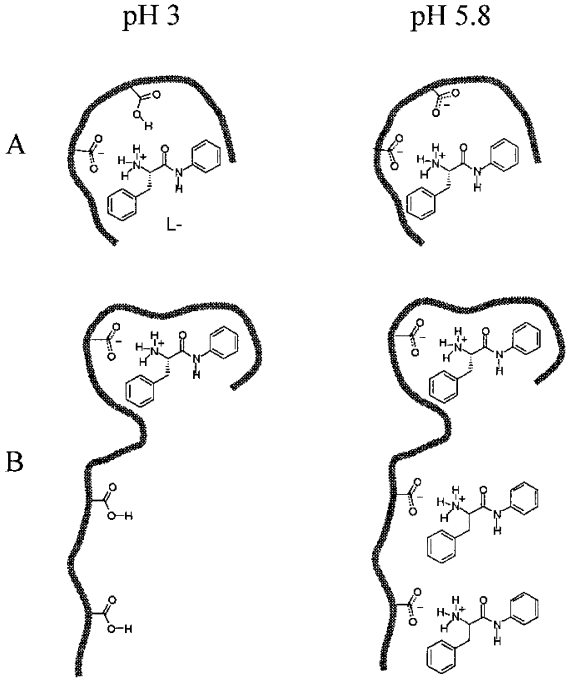

Scheme 1. Schematic representation of a molecule of L-PA adsorbed on imprinted sites of the polymer at different pH values.

Besides the polymeric network structure, its conformation appears to be important. Thermal treatments are required to achieve good chromatographic performance. They increase the column efficiency and reduce the extent of peak tailing. The influence of different thermal treatments of the imprinted polymers on the thermodynamics and kinetics of the retention processes of L- and D-PA was previously investigated at a mobile phase pH=5.8 [14].

In a previous study of an L-PA imprinted stationary phase, it was found that the retention data could be well fitted to a simple electrostatic retention model [11]. This model suggests a maximum of the retention factor at a pH close to the apparent pK_a of the solute and a rapid drop of the selectivity when the pH exceeds this value. Better to understand the role of the buffer pH in chiral separations on imprinted polymers, we made a study similar to our previous one [14] and measured the equilibrium isotherms of these two enantiomers at three different pHs, on the same annealed stationary phase. The purpose of this work is to report on these results, to describe the process followed for the selection of the best isotherm model, and to discuss the influence of the mobile phase pH on the isotherm parameters. Conclusions are then derived regarding some of the properties of the retention mechanisms involved.

2. Theoretical

We assume that the surface of the imprinted polymer is covered by two types of sites, the achiral or nonselective sites and those that are chiral or enantioselective. Such a model was successively used to account for equilibrium data in many enantiomeric separations [12,14,15]. In contrast with the chiral selective phases made of immobilized proteins, the chiral sites on imprinted polymers are much less homogeneous by design. This complicates the modeling and the interpretation of the experimental data.

Consistent with earlier findings [14], the experimental equilibrium data for D- and L-PA were first fitted to the bi-Langmuir isotherm model:

$$q_D^*(C_D) = \frac{a_1 C_D}{1 + b_1 C_D} + \frac{a_2' C_D}{1 + b_2' C_D} \quad (1)$$

$$q_L^*(C_L) = \frac{a_1 C_L}{1 + b_1 C_L} + \frac{a_2 C_L}{1 + b_2 C_L} \quad (2)$$

where q^* is the sample concentration in the stationary phase at equilibrium with the solution, C_D and C_L the concentration of each enantiomer in the mobile phase (with $C = C_D + C_L$), a_1, b_1, a_2, a_2', b_2, and b_2' numerical parameters. The first term accounts for the adsorption of the two enantiomers on the nonselective sites, with which they interact identically, while the template molecules (L-PA) interact more strongly than those of the other enantiomer with the selective sites. In some cases, $a_2' = b_2' = 0$ [14]. Then, only the molecules of L-PA interact with the enantioselective sites, not the molecules of D-PA.

The isotherm model in Eqs. (1) and (2) applies well to chiral separations on immobilized proteins because (1) the Langmuir model assumes that the adsorbent surface is homogeneous [16]; (2) although the adsorption energy distribution on the nonselective sites is not narrow, the adsorption energy on these sites is low [16]; and (3) proteins have a well defined structure and adsorption on their enantioselective sites has a narrow energy distribution [17,18]. Recent results show that this last assumption is not valid for imprinted polymers which have a more random structure and a wider adsorption energy distribution [19]. So, we used for each of the two types of sites a model that was recently shown [20] to account well for the adsorption of solutes on nonhomogeneous surfaces, the Jovanovic–Freundlich model:

$$q_D^*(C_D) = q_{s,1}\left(1 - e^{(a_1 C_D)^{\nu_1}}\right) + q_{s,2,D}\left(1 - e^{(a_2 C_D)^{\nu_2}}\right) \quad (3)$$

$$q_L^*(C_L) = q_{s,1}\left(1 - e^{(a_1 C_L)^{\nu_1}}\right) + q_{s,2,L}\left(1 - e^{(a'_2 C_L)^{\nu_2}}\right) \quad (4)$$

where $q_{s,1}$, $q_{s,2,D}$ and $q_{s,2,L}$ are the saturation capacities of the corresponding sites or solid-phase concentration corresponding to a monolayer (with $q_s = a/b$ for a Langmuir model), and a_1, a_2, a_2', ν_1, and ν_2 are numerical parameters. The parameters ν_1 and ν_2 characterize the degree of heterogeneity of the corresponding sites ($\nu = 1$ for a homogeneous surface). The first term in these two equations account for adsorption of either enantiomer on the nonselective type-I sites. The second one accounts for their adsorption on type-II enantioselective sites and, accordingly, the coefficients $q_{s,2,D}$ and $q_{s,2,L}$, on the one hand, a_2 and a_2' on the other, are different.

The values of the Fisher parameter (cf. Section 3.3.4) corresponding to the fit of the experimental data to the various isotherm models were calculated as explained previously [19]. The data are reported later.

3. Experimental

The same equipment, methodology, and procedures were used in this work and in the one previously reported [14]. Thus, only a brief account of the salient features is given, with emphasis on the minor adjustments made.

3.1. Equipment

An HP 1090 Series II system (Agilent, formerly Hewlett–Packard, Palo Alto, CA, USA) was used throughout the entire series of experiments. It consists of a multi-solvent delivery system, allowing solvent gradient or the delivery of a binary mobile phase of constant composition, an automatic injec-

tion system, a diode array UV detector, a column oven and a data system. The detector signals (chromatograms) were uploaded to a computer of the UT Computer Center for further calculations.

3.2. Mobile phase and samples used in the experiment

The mobile phase was a 70:30 (v:v) mixture of pure acetonitrile and an aqueous buffer (0.03 *M*). Buffers were prepared by dissolving in pure water the proper amounts of potassium phosphate and phosphoric acid in order to obtain values of the pH of 3.0 and 7.0. The pH was measured using a calibrated pH meter (American pH II). At each pH setting, solutions of D- and L-PA enantiomers were prepared at three different concentrations, 1.0, 0.1 and 0.01 g/l. The analyte samples were dissolved in the mobile phase solution. The samples and the buffer solution were filtered through 0.45 μm Nylon filters (Nalgene Filterware, NYL 150-0045, Nalgene, NY, USA) before applying to the instrument.

The samples, D- and L-phenylalanine anilide, were prepared by condensation of D- or L-phenylalanine with aniline [21].

3.3. Experimental procedures

3.3.1. Stationary phase

The preparation of the packing material was described earlier [10,11]. The amount of pure L-PA used to imprint the stationary phase used in this work was 57 mg/g of packing material produced. Effective imprinted stationary phases were later prepared with 20 and 50 times smaller proportions of L-PA. The selectivity remains high but the saturation capacity decreases in approximate proportion to the amount of L-PA used for imprinting them.

3.3.2. Column characteristics

As in earlier studies, the stationary phase was packed in a 0.46×10 cm stainless steel tube. The column efficiency, *N*, was measured before, during, and after all series of frontal analysis measurements. It was measured by injecting acetone, a non-retained tracer, at 40°C. This efficiency remained constant, at approximately 800 theoretical plates, throughout the entire set of experiments. At pH=5.8, the column efficiencies measured from the peak-width at half-height were 340 and 60 theoretical plates for D-PA and L-PA, respectively. The tailing factors (ratio of the rear to the front half peak-widths at 10% peak height) were 1.0, 1.6, and 2.4 for acetone, D-PA, and L-PA, respectively. A typical chromatogram of the racemic mixture is shown in Fig. 1.

The hold-up time of the column, t_o, was 0.916 min at pH=3.0 and 0.908 min at pH=7.0. The extra-column hold-up time, t_x, was measured by injecting acetonitrile after having replaced the column by a zero-dead volume connection. It was 0.937 min at pH 3.0, and 0.673 min at pH 7.0. The difference between these last two values of the hold-up time was caused by the change of a part of the instrument after the end of the first half of the experiments (maintenance).

3.3.3. Analytical retention

In order to set a proper time-table for the frontal analysis measurements, an analysis of both enantiomers was performed. Ten microliter samples of D-PA or L-PA were injected separately at 40°C, with a flow-rate of 1 ml/min. This served two purposes. First, the retention time of each analyte was used to determine the duration of each step for the FA experiments. Second, the analytical retention and separation factors were derived from these chromato-

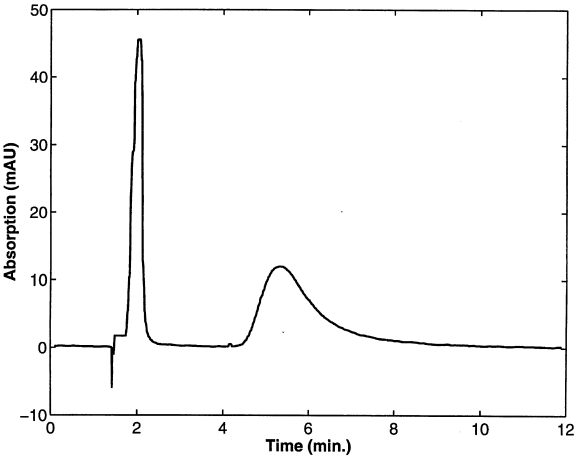

Fig. 1. Chromatogram of the PA racemic mixture on the imprinted stationary phase. Sample 50 nmole, mobile phase, MeCN/water/HOAc, 92.5:2.5:5 (v:v:v).

Table 1
Analytical retention of D-PA and L-PA[a]

Isomer	t_R (pH=3.0) min	t_R (pH=5.8) min	t_R (pH=7.0) min
D-PA	3.81	7.66	3.30
L-PA	9.06	21.80	4.12
α_{app}	2.82	3.10	1.32

[a] Sample size=10 μl. Concentrations (g/l), pH=3.0, D-PA, 0.02; L-PA, 0.08. pH=5.8, D-PA, 0.01; L-PA 0.1. pH=7.0, D-PA, 0.01; L-PA, 0.05.

grams. The data displaying the effect of the pH at infinite dilution are shown in Table 1.

3.3.4. Recording of breakthrough curves

A procedure involving a 10-step staircase FA up to a concentration of 0.01 g/l, followed by a seven-step staircase to the concentration of 0.1 g/l, and, finally, by a second seven-step staircase to 1 g/l, was followed for both enantiomers at each temperature. This gave 24 data points for each analyte at each temperature and pH. However, it was not possible to observe a well defined initial step for the more retained enantiomer, L-PA. The step recorded at the lowest concentration was very wide and diffuse (NB. This observation is consistent with an energetically heterogeneous surface, see later). Therefore, there are only 23 data points for this component in each series. All the FA experiments were conducted by going from low to high concentrations. The column was equilibrated before each new experiment. All the required measurements at pH=3.0 were first performed at 40°C and then continued successively at 50, 60 and 70°C. The flow-rate was maintained at 1 ml/min during the entire series of experiments. After finishing the measurements at pH=3.0, a new pH buffer was made at pH=7.0 and the entire procedure was repeated. The signals were detected at wavelengths of 260 and 280 nm by the UV detector. The first wavelength was used at low concentrations, the second at high concentrations.

3.3.5. Fitting of the experimental data to the isotherm models

The nonlinear regression analysis of the models was done using a fitting procedure based on Marquardt algorithm which minimizes the residual sum of the squares of the differences between the experimental data and the model calculations. The estimates of the parameters present in the models are given at the asymptotic 95% confidence interval. For each model and each set of experimental data, the Fisher parameter was calculated according to [22]:

$$F_{calc} = \frac{m-l}{m-1} \frac{\sum_{i=1}^{m} (q_{exp,i} - \overline{q_{exp}})^2}{\sum_{i=1}^{m} (q_{exp,i} - q_{t,i})^2} \quad (5)$$

where $q_{exp,i}$ are the experimental values of the solid-phase concentration of the adsorbate for a given system, $\overline{q_{exp,i}}$ is the mean value of the data, $q_{exp,i}$, for a given system, $q_{t,i}$ are the estimate of the solid-phase concentration of the adsorbate by a given model, l is the number of adjusted parameters in the model, and m is the number of experimental data for a given system.

4. Results and discussion

4.1. Retention at infinite dilution

Table 1 lists the retention times of D-PA and L-PA at infinite dilution under various pH conditions. The largest retention times for both enantiomers were measured at pH=5.8, close to the pK_a of the analytes. This behavior was explained by an electrostatic retention model [11]. At pH 5.8, this mechanism would be an ion-exchange process. Its contribution to the retention factor of an analyte, proportional to the product of the degree of ionization of this analyte and of the stationary phase, is maximum. The separation factor is also maximum at pH 5.8. However, it is better to carry out the analyses at pH=3.0 because the retention times are shorter while the separation is nearly as easy.

The retention data at pH=7.0 indicates that the selective binding sites are severely deactivated. The separation factor of L-PA and D-PA is low (1.32). The most probable reason for this to happen is that the ratio of the numbers of nonselective and selective sites increases significantly at high pH, because the first number increases, the second one decreases, or for any combination of these two causes. This would explain why the separation ability of the stationary phase decreases: the dramatic decrease of the relative density of the enantioselective sites reduces their

influence. A more detailed discussion is found elsewhere [11].

4.2. Retention at finite concentrations

The two isotherm models (Eqs. (1), (2) and (3), (4), respectively) can be applied in two different ways, as fitting equations for experimental data or as an actual physical model of the equilibrium observed. An excellent fit of experimental data to the equations of a model is never a demonstration of the physical validity of this model. Therefore, the interpretation of the results must always be cautious. In the following, we discuss first the results obtained by fitting the experimental data to different versions of the two models described in the theory section. Later, we derive some conclusions from the sets of parameters calculated.

Several simplifications may be introduced in the two models described earlier, depending on the characteristics of the stationary phase studied [14]. For the bi-Langmuir model, we can distinguish four different cases [15,18,19]. First, the eight coefficients of the bi-Langmuir isotherms of the two enantiomers can be different. In this case, none of the Langmuir terms account purely for nonselective interactions. The influence of nonselective and enantioselective interactions cannot be separated simply and the isotherm obtained is completely empirical. This could be consistent with an overlap of the adsorption energy distributions of the two types of sites, the adsorption energy on the strongest type-I sites being higher than that on the weakest enantioselective sites which is suggested by some independent results [17]. Second, the set of Eqs. (1) and (2) is valid and six coefficients are obtained. In this case, enantioselective and nonselective interactions are separated and their thermodynamics can be studied separately. The two enantiomers interact, albeit with different Gibbs free energies, with the chiral sites (or, possibly, they interact with different chiral sites, a remote possibility in the present case since the template was a pure enantiomer). Third, the saturation capacities for the two chiral terms are the same. This would suggest that both enantiomers interact with the same chiral sites. In this case, there are only five different parameters. Fourth, the coefficient b of the enantioselective term in the isotherm of D-PA is zero. This compound does not interact with the cavities imprinted by its enantiomer, which is possible, if not probable. This model has only four independent parameters. We consider this last model as the most physically meaningful in the case studied. So, because of all the physical considerations reported above, the experimental data were fitted to two of these models only, the eight-parameters and the four-parameters bi-Langmuir isotherm models. The latter was already successfully used at pH = 5.8 in a previous study of the same packing material [14].

Similarly, several assumptions can be made regarding the Jovanovic–Freundlich model. Besides the general case corresponding to Eqs. (3) and (4), two simplified models seem to be reasonable and worth considering. First, the nonselective sites may behave as a homogeneous surface, with $\nu_1 = 1$, the corresponding contribution reducing to a pure Jovanovic isotherm, practically very close to a Langmuir term [20]. Second, there may be no selective interactions between the type-II sites and the D-enantiomer, the enantiomer of the template. In this case, the corresponding saturation capacity would become negligible ($q_{s,2,D} = 0$). In this work, the data were fitted only to the simplified Jovanovic–Freundlich model shown in Table 4. It assumes that the D-PA molecules do not interact with the imprinted sites.

In the interpretation of the results obtained, we must weigh the fact that the larger the number of parameters of a model, the higher its flexibility, and the best the fit that it is bound to give. To select the best model on a scientific basis, all the data were fitted to the different models described above and the Fischer test [19] was applied. We must stress, however, that, by demanding that the model selected has a physical sense, we impose an additional constraint. If not quantitative, this constraint remains quite significant. Accordingly, a physically meaningful model may account less well for the experimental data than a purely empirical model.

Note finally that, to check and compare the validity of the different models discussed above, we must first carry out the nonlinear fitting of the experimental data to the equations representing the physical models just described. Conventional numerical algorithms are used for the calculations of the best estimate of the equation coefficients, their

reliability, and the values of the Fisher test. As explained elsewhere [18], these algorithms allow the accurate identification of the coefficients of the isotherm models such as those used here (Eqs. (1)–(4)), only if the equilibrium constants corresponding to the two types of sites differ by at least an order of magnitude (in agreement with the assumption of the coexistence of two very different retention mechanisms). Otherwise, the numerical derivation of the best isotherm coefficients becomes indeterminate or extremely inaccurate. As a consequence, the experimental data must be acquired in a range of concentration spanning at least three orders of magnitude.

4.3. Fitting the experimental data to the isotherm models

The frontal analysis data (symbols) are reported in Fig. 2 (pH = 3.0) and Fig. 3 (pH = 7.0) in logarithmic plots. This type of plot allows an easy visual presentation of all the data acquired. However, the use of logarithmic coordinates significantly reduces the apparent curvature of the plots obtained (cf. Figs. 2 and 3 and further figures). The lines shown in each figure are the best fit of the experimental data to the best model (see later discussion). The best estimates of the numerical coefficients of the isotherm model equations were determined as explained in Section 3.3.4. and are reported in Table 2 (eight-parameters bi-Langmuir model), Table 3 (four-parameter bi-Langmuir model) and Table 4 (six-parameter bi-Jovanovic–Freundlich model).

The difference between the results of the two series of measurements is obvious. At pH = 3.0, there is almost no temperature influence on the isotherm, either for D-PA or for L-PA. By contrast, at pH = 7.0 (as previously reported at pH = 5.8 [14]), the amount of L-PA adsorbed at equilibrium with a given mobile phase concentration decreases steadily with increasing temperature (Fig. 3), by a factor of approximately 2.3 between 40 and 70°C at pH = 7.0, versus 3.7 at pH = 5.8 (see Ref. [14] and Tables 2 and 3). Thus, the isotherms of each enantiomer at increasing temperatures are lower and lower in the figure. These results are in qualitative agreement with a previous report on the temperature dependence of the retention at infinite dilution on L-PA-imprinted stationary phases [23].

The influence of the pH on the isotherms of D- and L-PA is illustrated in Fig. 4, using only the data at 40°C, for the sake of simplicity. The isotherm data at pH = 3.0, 5.8 [14] and 7.0 are shown in Fig. 4a–c, respectively. At a given mobile phase concentration, the stationary phase concentration of L-PA at equilibrium is always higher than that of D-PA, as expected since the stationary phase is L-PA imprinted. The distance between the isotherms of L-PA and D-PA decreases with increasing buffer pH and so does the resolution between their peaks. At pH = 7.0 the L-PA and D-PA data are almost superimposed and the resolution between the bands of the two enantiomers is very small (see Table 1). By contrast, the separation is easy at both low pHs, 3.0 and 5.8. Finally, Fig. 4 confirms that the separation of D-PA and L-PA is best at low concentrations. This arises because adsorption is stronger on the enantioselective than on the nonselective binding sites. The former sites become saturated at low concentrations and leave only nonspecific sites available. No separation can be achieved on these sites.

Figs. 5 and 6 show the L-PA isotherm data at pH = 3.0 and pH = 7.0, respectively, in conventional coordinates, in the whole concentration range (the same data at pH = 5.8 are in Ref. [14]). Obviously, the data at pH = 7.0 are nearly linear. Fitting of these data to a simple Langmuir isotherm indicates a very slight curvature, the nonlinear term, bC, being always less than 0.02. This shows that all the data were measured in the linear range of the isotherm [15]. This arose from the limited solubility of the PA isomers that prevented data acquisition at higher concentrations. Accordingly, the data at pH = 7.0 could not be included in the isotherm modeling. Fitting the experimental data at pH = 3.0 and 5.8 to the models discussed earlier gave the sets of isotherm coefficients reported in Tables 2–4.

4.3.1. Eight-parameters bi-Langmuir model

The best values of the parameters of this model are reported in Table 2. In this case, the coefficients a_1 and b_1 correspond to the type of sites that are closest for the two enantiomers and a_2 and b_2 to the most different type, respectively. Small fitting residuals are obtained at pH = 3.0 (Table 2). The

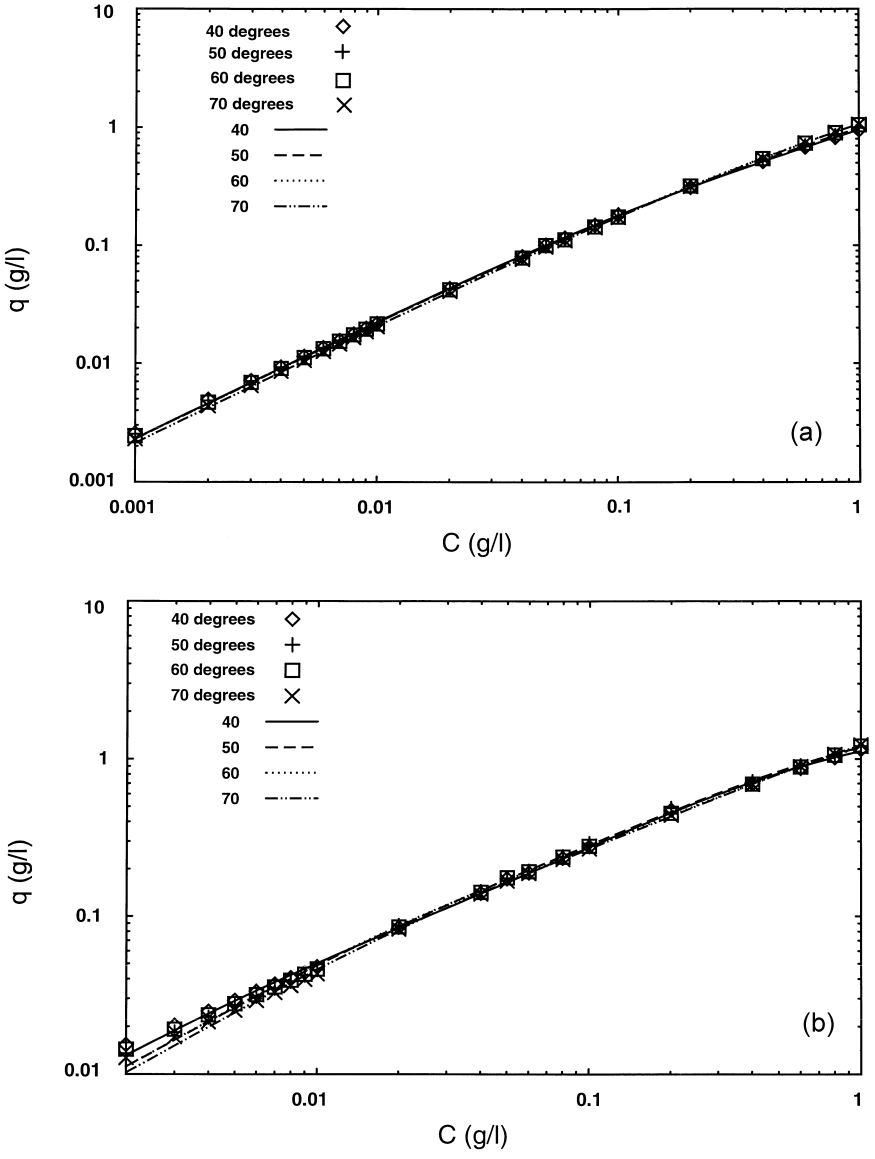

Fig. 2. Experimental isotherm data for the enantiomers of phenylalanine anilide (PA) on the imprinted polymer at 40, 50, 60 and 70°C at pH = 3.0. Logarithmic coordinates. The interpolating lines in all figures show the best isotherms. (a) Data for D-PA. (b) Data for L-PA.

isotherms measured at pH 3.0 are strongly curved at intermediate and high concentrations, indicating that saturation of the most strongly enantioselective sites was reached and that the nonselective sites were also beginning to saturate. This later statement is confirmed by the maximum values of b_2C ranging between 0.20 and 1.0 for L-PA, depending on the temperature. These values correspond respectively to 17% and 50% of monolayer coverage.

4.3.2. Four-parameters bi-Langmuir model

The best values of the parameters for this model are reported in Table 3. The results previously

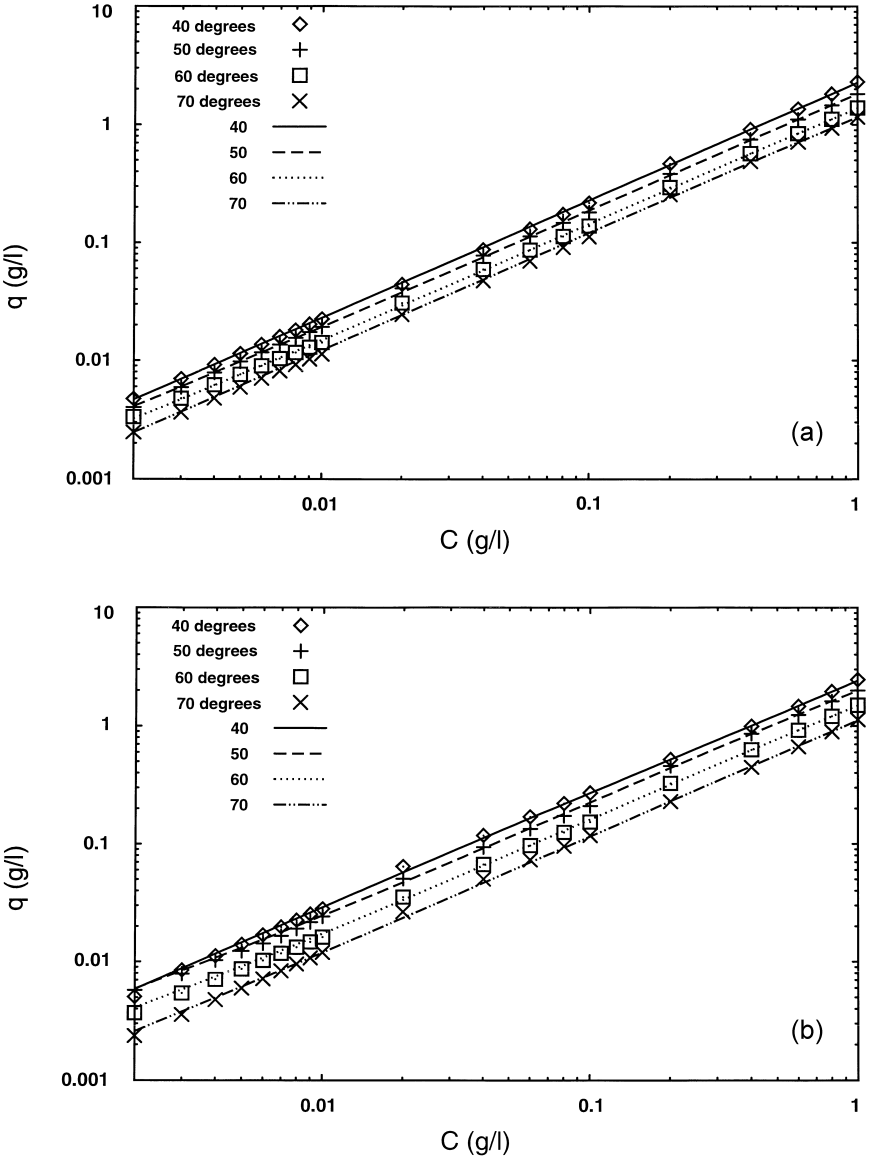

Fig. 3. Experimental isotherm data for the enantiomers of phenylalanine anilide (PA) on the imprinted polymer at 40, 50, 60 and 70°C at pH = 7.0. Logarithmic coordinates. (a) Data for D-PA. (b) Data for L-PA.

reported at pH = 5.8 were consistent with this model [14]. The results at pH = 3.0 are different. The residuals obtained with this model for L-PA are two to three times larger than with the previous model and the *F*-test suggests that it is significantly less satisfactory. Yet, these residuals are small. So, although the experimental results are more consistent with the previous model, the simpler four-parameters bi-Langmuir model should still be preferred because of its clear physical meaning. Adopting the eight-parameter bi-Langmuir model would suggest that a change of pH has a profound influence on the retention mechanism. The evidence in the data is not sufficiently compelling to warrant this conclusion.

Table 2
Eight-parameter bi-Langmuir model fittings and residuals

pH = 3.0 T (°C)	L-PA				D-PA				Fitting residuals × 10^4	
	a_1	b_1 (l/g)	a_2	b_2 (l/g)	a_1	b_1 (l/g)	a_2	b_2 (l/g)	L-PA	D-PA
40	2.63± 0.15	1.45± 0.13	4.68± 0.53	92.4± 29.8	0.97± 0.09	0.30± 0.07	1.35± 0.08	5.58± 0.68	32	3
50	2.30± 0.18	1.10± 0.14	3.51± 0.24	35.5± 8.8	1.26± 0.08	0.45± 0.06	1.04± 0.07	8.07± 1.45	34	3
60	1.84± 0.14	0.74± 0.11	3.98± 0.19	27.9± 4.7	1.42± 0.06	0.46± 0.04	0.85± 0.05	10.60± 1.90	29	3
70	1.73± 0.10	0.60± 0.08	3.54± 0.13	23.4± 3.1	1.33± 0.07	0.38± 0.05	0.80± 0.06	6.90± 1.30	17	2

Best parameters for a fit of the data to the following model: $q_D^*(C_D)=\frac{a_1' C_D}{1+b_1' C_D}+\frac{a_2' C_D}{1+b_2' C_D}$; $q_L^*(C_L)=\frac{a_1 C_L}{1+b_1 C_L}+\frac{a_2 C_L}{1+b_2 C_L}$

4.3.3. Bi Jovanovic–Freundlich model

The best values of the parameter of this model are reported in Table 4. The residuals obtained at pH = 3.0 are extremely small, much lower than for any form of the bi-Langmuir isotherm. Similar calculations performed with the data obtained at pH = 5.8 also gave low residuals. For these reasons, this model is better than either bi-Langmuir model. This conclusion is satisfactory because the biJovanovic–Freundlich model makes more physical sense than a bi-Langmuir model. The values obtained for the saturation capacities of the two types of sites and the surface heterogeneity are discussed later. Clearly, the structure of the stationary phase is strongly suggestive of an energetically heterogeneous surface, in agreement with other results [17].

4.3.4. Simple Jovanovic–Freundlich model

The best values of the parameters of a simple Jovanovic–Freundlich isotherm are given in Table 5.

Table 3
Four-parameter bi-Langmuir model fittings and residuals

T (°C)	L-PA						D-PA		Fitting residuals × 10^4	
	a_1	b_1 (l/g)	q_{s1} (g/l)	a_2	b_2 (l/g)	q_{s2} (g/l)	a_1	b_1 (l/g)	L-PA	D-PA
pH = 3.0										
40	2.10± 0.06	1.17± 0.08	1.8	5.13± 0.52	47.3± 8.2	0.11	2.10± 0.06	1.17± 0.08	190	200
50	2.00± 0.05	1.08± 0.06	1.8	4.22± 0.33	29.2± 4.0	0.14	2.00± 0.05	1.08± 0.06	150	140
60	1.95± 0.03	0.88± 0.04	2.2	3.96± 0.23	28.2± 2.7	0.14	1.95± 0.03	0.88± 0.04	60	84
70	1.88± 0.03	0.78± 0.03	2.4	3.49± 0.19	24.7± 2.3	0.14	1.88± 0.03	0.78± 0.03	50	66
pH = 5.8										
40	6.50± 0.10	0.36± 0.03	18	4.70± 0.50	10.0± 2.0	0.45	6.50± 0.10	0.36± 0.03	470	170
50	4.55± 0.08	0.27± 0.03	17	2.40± 0.70	8.0± 2.0	0.30	4.55± 0.08	0.27± 0.03	240	170
60	2.73± 0.05	0.05± 0.02	50	1.90± 0.20	6.0± 1.0	0.30	2.73± 0.05	0.05± 0.02	220	57
70	2.02± 0.03	0.01± 0.02	n.a.	0.93± 0.08	4.4± 0.8	0.20	2.02± 0.03	0.01± 0.02	67	44

Best parameters for a fit of the data to the following model: $q_D^*(C_D)=\frac{a_1 C_D}{1+b_1 C_D}$; $q_L^*(C_L)=\frac{a_1 C_L}{1+b_1 C_L}+\frac{a_2 C_L}{1+b_2 C_L}$: n.a., not applicable.

Table 4
Bi-Jovanovic–Freundlich model fittings and residuals

T (°C)	Enantioselective sites			Nonselective sites			Fitting residuals $\times 10^4$	
	$q_{s,2,L}$ (g/l)	$a_{2,L}$	ν_2	$q_{s,1}$ (g/l)	a_1	ν_1	L-PA	D-PA
pH = 3.0								
40	1.88	0.66	0.85	0.20	7.43	0.84	2.80	6.40
50	2.00	0.64	0.87	0.22	7.29	0.85	2.00	6.20
60	2.19	0.61	0.89	0.16	11.30	0.80	1.07	1.55
70	2.38	0.55	0.90	0.16	8.83	0.77	0.89	1.74
pH = 5.8								
40	8.58	0.79	1.02	0.79	1.43	0.62	75	19
50	8.34	0.56	1.03	0.61	0.99	0.60	51	42
60	11.20	0.27	1.03	1.11	0.185	0.58	14	51
70	11.80	0.195	1.04	1.43	0.049	0.60	17	17

Best parameters for a fit of the data to the following model: $q_D^*(C_D) = q_{s,1}\left(1 - e^{(a_1 C_D)^{\nu_1}}\right)$; $q_L^*(C_L) = q_{s,1}\left(1 - e^{(a_1 C_L)^{\nu_1}}\right) + q_{s,2,L}\left(1 - e^{(a'_2 C_L)^{\nu_2}}\right)$

Although the residuals are slightly larger than in the previous case, the Fisher test gives comparable (pH = 5.8) or even lower (pH = 3.0) values because there are fewer parameters. This result confirms that the surface is heterogeneous and suggests that the precision and accuracy of the data may not justify the use of more complex isotherm models.

4.3.5. Model selection

The values of the Fisher coefficients are listed in Table 6. They suggest that the best results are obtained with the six-parameter biJovanovic–Freundlich isotherm (the D-enantiomer not interacting with the enantioselective sites). This model is only slightly better than the simpler Jovanovic–Freundlich isotherm with the same number of parameters. The advantage of the former model over the latter one is its stronger theoretical justification.

4.4. Saturation capacities

The saturation capacity is a direct parameter of the Jovanovic–Freundlich isotherm model. For the Langmuir isotherm, it is the ratio of the two coefficients *a* and *b*. Values for the four-parameter bi-Langmuir isotherm are also included in this discussion to illustrate the difficulties and ambiguities associated with the derivation of proper conclusions from the results of a successful modeling of isotherm data.

The data in Table 3 show that an increase in the mobile phase pH causes a strong increase in the saturation capacity of both types of sites. The saturation capacity of the chiral sites is nearly twice larger at pH = 5.8 than at pH = 3.0, at all the temperatures studied. The saturation capacity of the nonselective sites increases by one order of magnitude when the pH increases from 3.0 to 5.8 (Table 3). At pH = 3.0, the saturation capacities of the nonselective and the enantioselective sites is nearly independent of the temperature, which is consistent with the small temperature dependence of the isotherms at this pH (Table 3). At pH = 5.8, by contrast, the saturation capacity of the nonselective sites more than doubles between 40 and 70°C, although the highest temperature data are imprecise. Note, finally, that the saturation capacity of the chiral sites is always ten to twenty times lower than that of the nonselective sites.

Obviously, the same conclusions are reached from a discussion of the values of the saturation capacities afforded by the bi-Jovanovic–Freundlich isotherm model (Table 4). The saturation capacity of the nonselective sites is an order of magnitude larger than that of the enantioselective sites. Both saturation capacities vary little with temperature at pH = 3.0 and increase with increasing temperature at pH = 5.8. The saturation capacity of the enantioselective sites is higher at pH = 5.8 than at pH = 3.0. All results confirm that the low energy sites outnumber the high energy sites by an order of magnitude at pH 5.8 as well as at pH 7.0. With both composite isotherm

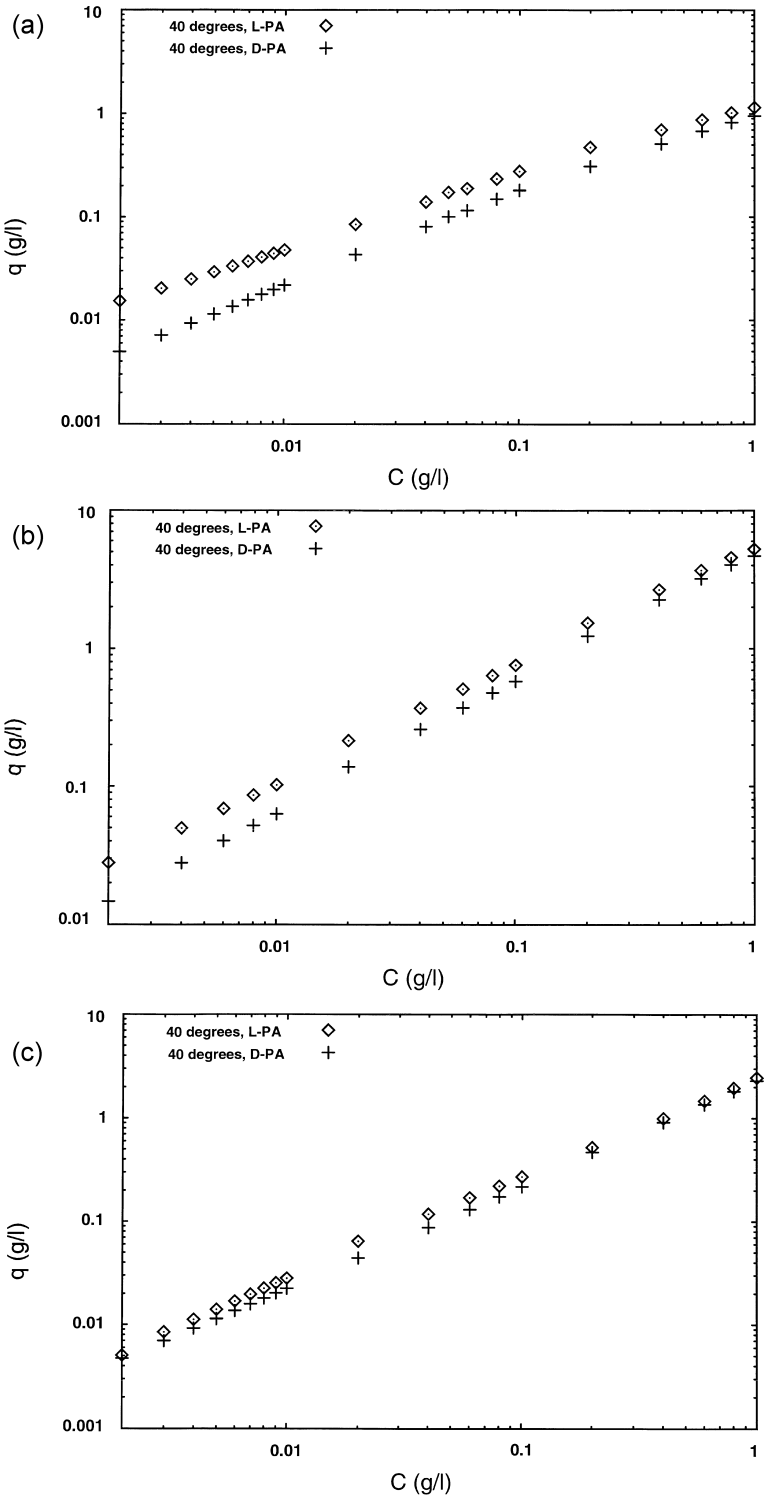

Fig. 4. Comparison between the experimental isotherm data of L-PA and D-PA at 40°C. Data at pH = 3.0 and 7.0 (this work) and at pH = 5.8 [14]. Symbols, ◇ for L-PA, + for D-PA. (a) pH = 3.0; (b) pH = 5.8; (c) pH = 7.0.

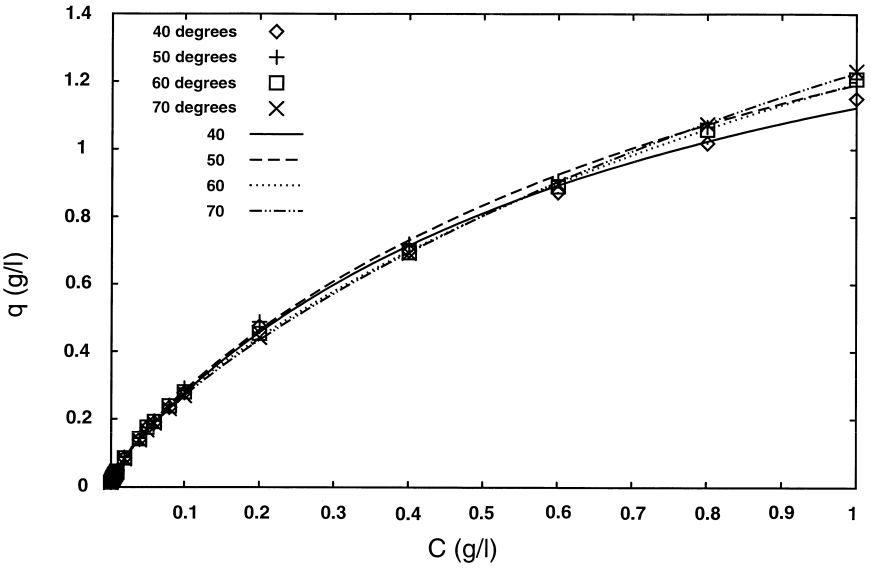

Fig. 5. Isotherms of L-PA at pH = 3.0, in conventional coordinates.

models, the second contribution appears to be a correction to the primarily one, itself reasonably well accounted for by the Langmuir model. This is not a surprising result.

4.5. Surface homogeneity

The data in Table 4 show that, at pH = 5.8, the first type of sites is nearly homogeneous ($1.0 < \nu < 1.04$).

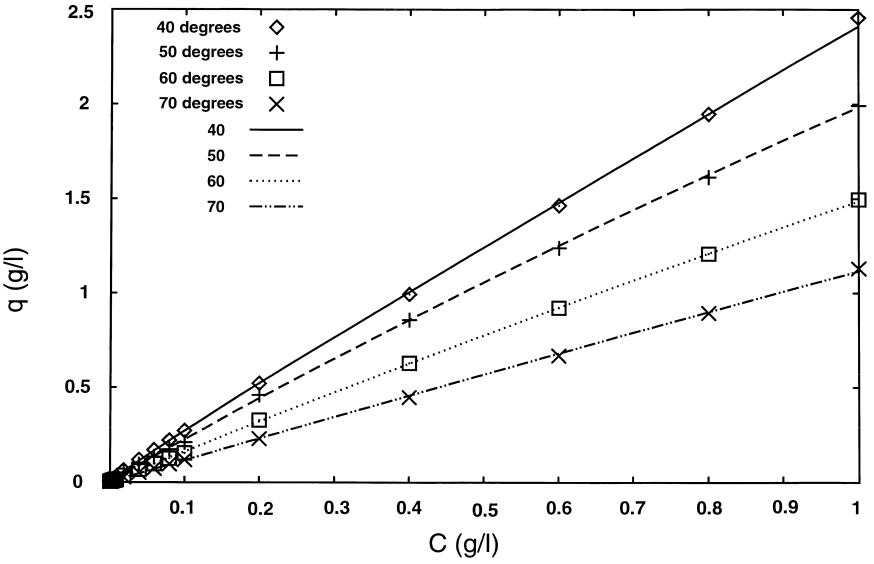

Fig. 6. Isotherms of L-PA at pH = 7.0, in conventional coordinates.

Table 5
Jovanovic–Freundlich model fittings and residuals

T (°C)	D-PA			L-PA			Fitting residuals $\times 10^4$	
	$q_{s,D}$ (g/l)	a_D	ν_D	$q_{s,L}$ (g/l)	a_L	ν_L	L-PA	D-PA
pH = 3.0								
40	1.78	0.72	0.86	1.86	0.93	0.77	9	3
50	1.91	0.69	0.87	1.98	0.91	0.78	11	2
60	1.98	0.72	0.91	2.86	0.44	0.73	5	2
70	2.29	0.59	0.90	2.64	0.54	0.77	5	1
pH = 5.8								
40	8.77	0.77	1.01	11.0	0.62	0.91	203	74
50	11.60	0.36	0.98	11.8	0.38	0.92	49	67
60	11.30	0.26	1.03	12.7	0.24	0.94	72	13
70	11.50	0.20	1.04	12.4	0.19	0.98	33	16

Best parameters for a fit of the data to the following model: $q_D^*(C_D) = q_{s,D}\left(1 - e^{(a_D C_D)^{\nu_D}}\right)$; $q_L^*(C_L) = q_{s,L}\left(1 - e^{(a_L C_L)^{\nu_L}}\right)$

In this case, a simple Jovanovic or Langmuir isotherm model would account as well for the adsorption behavior of the PA enantiomers on the nonselective sites [20]. This is no longer true at low pH. A value of $\nu_1 = 0.85$–0.90 indicates that the surface is already rather heterogeneous.

By contrast, the homogeneity of the second type of sites appears to be higher at pH = 3.0 than at pH = 5.8. While at pH = 3.0, these sites are barely more heterogeneous than the nonselective sites (with $\nu_2 = 0.80$–0.85 instead of $\nu_1 = 0.85$–0.90), they become strongly heterogeneous at pH = 5.8, with $\nu_2 = 0.60$. This suggests that improved results at moderate or high pH could be obtained by using, in the synthesis of the polymer, monomers having higher pK_a values. It is noteworthy that the saturation capacity of the selective sites increases four to eight times when the pH increases from 3.0 to 5.8 at the same time that the heterogeneity factor drops from 0.8 to 0.6. It seems that increasing the pH in this range activates new sites and that, in the same time, the adsorption energy distribution broadens. Thus, the adsorption energy distribution is probably correlated to a surface pK_a distribution.

4.6. Retention mechanism

The pH of all aqueous buffer solutions were carefully measured before mixing them with acetonitrile. The exact values of the pH of the three mobile phases used in this work were 3.0, 5.8 and 7.0. However, it is well known that the pH of a solution shifts when it is mixed with an organic solvent [24–26]. In our experiments, the apparent pH of the

Table 6
Fisher parameters for the different isotherm models studied

pH	Model	Number of degrees of freedom	Fisher values (40°C)	
			D-PA	L-PA
3.0	Jovanovic–Freundlich	6	4900	2400
3.0	bi-Jovanovic–Freundlich	6	930	2600
3.0	bi-Langmuir	8	36 000	1630
3.0	bi-Langmuir	4	1480	1200
5.8	Jovanovic–Freundlich	6	4900	2100
5.8	bi-Jovanovic–Freundlich	6	4900	1800
5.8	bi-Langmuir	8	4500	2100
5.8	bi-Langmuir	4	1950	2300

mobile phase increases after mixing the buffer with acetonitrile. The true pH values were estimated to be about 4.0, 7.0 and 8.3, respectively [27]. The apparent pK_a of L-PA was measured at 6.4, and the average pK_a of the acid groups of the polymers was reported to be 8.9 for the imprinted sites and 9.3 for the blank, non-imprinted sites [11]. Using all this information, a qualitative understanding of the chemical environment of the adsorption sites at various pH values can be presented.

At low pH (pH = 3.0, pH_{app} = 4.0), the apparent pH of the mobile phase is much lower than the average pK_a of the carboxylic groups of the polymer (pK_a = 8.9 and 9.3). The major part of these acid groups are thus protonated and in the neutral form. The solute molecules are positively charged and interact mainly with those acid groups that are ionized. This would explain the low saturation capacity of both types of sites and the small values of the retention factors (see Table 1). At a buffer pH = 5.8 (corresponding to an apparent mobile phase pH = 7.0), the solute is only partly ionized. However, the fraction of the polymer acid groups that are ionized, hence the net negative charge of the polymer, is much higher and a high retention volume is observed [11]. At higher pH values, the solute loses its charge, it can no longer give ionic interactions with the stationary phase, and the retention factor decreases. However, the degree of ionization of the polymer increases, and more sites become available for adsorption at all energies (although the values of q_s at pH = 7.0 are questionable because of their imprecision, they do trend in this direction). When the pH increases from 3 to 5.8, the increase (10-fold) of the nonselective saturation capacity is twice larger than that of the selective one (see Section 4 and Table 3). This observation supports a model of retention mechanism which assumes that the acid groups of the selective sites are more acidic, hence ionized at a lower pH than the nonselective sites (see B in Scheme 1) [11]. This result fully explains the decrease in selectivity observed when the pH increases.

Structural changes at the selective sites may also contribute to the observed decrease in selectivity with increasing pH, as proposed in A, in Scheme 1. The importance of this factor is illustrated by the values of the binding energy (i.e., of the coefficients b_i) in Table 3 and of the site heterogeneity (measured by the coefficient ν) in Table 4. The bi-Langmuir coefficient b_2 decreases approximately five-fold when the pH increases from 3 to 5.8. The heterogeneity coefficient decreases markedly. Assuming that conformational changes of the polymer chain do not affect the binding site structure in this pH interval (the swelling factor did not change with the pH [11]), these results are most likely due to a loss of stabilizing hydrogen bonds arising from further site ionization. This is illustrated in Scheme 1(A).

As discussed earlier, the adsorption isotherms at pH = 3.0 are nearly independent of the temperature. This may be explained by the influence of the temperature on the hydration of the solute and the stationary phase at this pH. At pH = 3.0, ammonium ions are strongly hydrated, involving up to four shells of water molecules. Any interaction between the solvated ammonium groups of the solute and the solvated carboxylate groups of the binding sites requires desolvation of these groups. At pH = 3.0, most binding sites are occupied by water molecules sorbed through hydrogen bonding. When the temperature increases, more and more binding sites become available, because of the loss of the associated H_2O, providing a larger saturation capacity for the PA enantiomers. This effect compensates for the decrease of the amount adsorbed at equilibrium with increasing temperature. A similar temperature effect was reported earlier on a different system, involving the hydration of 2-propanol [28]. The dehydration process of the stationary phase can be described by the Boltzmann distribution law. By fitting the experimental data to this equation, a value $\Delta H^\circ = 4.4$ kcal/mol is derived for the enthalpy of desorption of H_2O, a result in excellent agreement with the hydrogen bond strength [29]. This supports the proposed explanation of the peculiar apparent lack of temperature dependence at pH 3.0.

This temperature dependence corresponds usually to increased entropy and enthalpy terms, possibly leading, in extreme cases, to an endothermic retention behavior [23]. This is illustrated by the Van't Hoff plots in Fig. 7. Linear plots suggest that a single retention mechanism is predominant [28]. The plots corresponding to the different types of sites are parallel and reasonably linear in the temperature

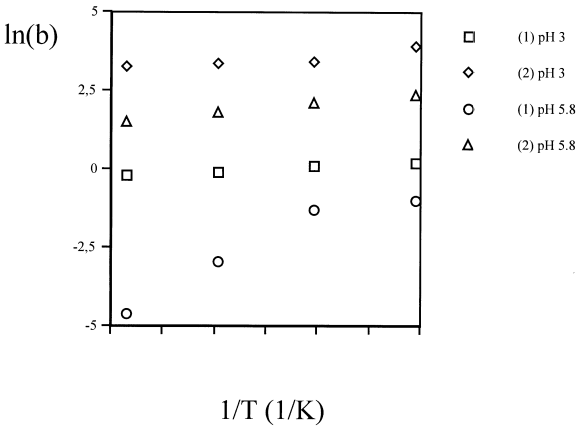

Fig. 7. Van't Hoff plots of the binding energy of the selective and the nonselective sites at pH=3 and pH=5.8. □, type-I sites at pH=3.0; ◇, type-II sites at pH=3.0; ○, type-I sites at pH=5.8; △, type-II sites at pH=5.8.

interval studied, except for the nonselective sites at pH 5.8. The slope of this last plot is larger than the others, suggesting that association to these sites is enthalpically driven. It is interesting to note that this does not apply to the selective sites at this pH. This result also agrees with our previous model proposing that the solute loses more of its solvation shell upon binding to selective sites than to nonselective sites [23].

5. Conclusion

A model of adsorption isotherm for heterogeneous surface accounts for the adsorption behavior of D- and L-phenylalanine anilide on a polymeric network imprinted for the L-enantiomer. This model assumes that the adsorbent surface contains nonselective and enantioselective sites. Both enantiomers are identically adsorbed on the nonselective sites. Only the molecules of the template, L-PA, are adsorbed on the enantioselective sites. The saturation capacity of both types of sites, their average adsorption energy and their degree of homogeneity depend on the pH of the mobile phase. Both saturation capacities increase with increasing pH. The saturation capacity of the nonselective sites calculated with the bi-Langmuir model increases more than that of the selective sites in the pH interval studied. The values derived from the Jovanovic–Freundlich model suggest that the ratio of these saturation capacities remains nearly constant and approximately equal to 10. Although this ratio could serve as a figure of merit to assess progress in the preparation of more selective materials, it might become more difficult to measure as the relative importance of chiral adsorption increases. While the nonselective part of the surface is almost homogeneous at pH=3.0 and completely so at pH=5.8, the enantioselective part of the surface (i.e., the imprinted sites) is heterogeneous at all pHs and its degree of homogeneity decreases with increasing pH (in the same time as the number of accessible such sites increases). These properties are explained by the relative values of the mobile phase pH and of the pK_a of the polymer acid groups and of the analytes. The binding energy given by the bi-Langmuir model for the selective sites decreases in this pH range.

Thus, the retention behavior of the stationary phase studied is explained by the relative values of the mobile phase pH and of the pK_a of the carboxylic acid groups of the polymer and that of the analytes. The pronounced increase observed in the number of nonselective sites with increasing pH is in agreement with a previously proposed retention model [23]. Furthermore,. the decrease of the binding energy of the solutes at the selective sites with increasing pH supports a binding site model involving more than one carboxylic acid groups per site. Ionization of one of these groups allows the positively charged ionized solute to interact electrostatically with the site while additional hydrogen bond stabilization is provided by a second nonionized acid group. Although other factors can account for this behavior, the data provides unique support for a binding site model in imprinted polymers.

Because of the limited solubility of phenylalanine anilide in the mobile phase at pH=7.0, it was not possible to measure the equilibrium isotherms in a range of concentrations within which these isotherms deviate strongly enough from linear behavior. This forbade the determination of accurate values of the isotherm coefficients. It is worth noting, however, that these measurements were made in the same concentration range at all the three pHs studied. This can only mean that the saturation capacities of the nonselective sites are larger at pH=7.0 than at pH=5.8 while their adsorption energies remain of the

same order of magnitude (or decrease). Although the separation factor decreases with increasing pH, operating in preparative chromatography at an intermediate pH appears attractive as it will lead to a higher production rate.

Acknowledgements

This work was supported in part by grant CHE-00-70548 of the National Science Foundation and by the cooperative agreement between the University of Tennessee and the Oak Ridge National Laboratory.

References

[1] B. Sellergren, Chirality 1 (1989) 63.
[2] L.I. Andersson, K. Mosbach, J. Chromatogr. 516 (1990) 313.
[3] O. Ramström, L.I. Andersson, K. Mosbach, J. Org. Chem. 58 (1993) 7562.
[4] C. Yu, K. Mosbach, J. Org. Chem. 62 (1997) 4057.
[5] S. Vidyasankar, M. Ru, F.H. Arnold, J. Chromatogr. A 775 (1997) 51.
[6] K. Yano, K. Tanabe, T. Takeuchi, J. Matsui, K. Ikebukuro, I. Karube, Anal. Chim. Acta 363 (1998) 111.
[7] K. Hosoya, Y. Shirasu, K. Kimata, N. Tanaka, Anal. Chem. 70 (1998) 943.
[8] O. Ramström, L. Ye, P.E. Gustavsson, Chromatographia 48 (1998) 197.
[9] I.A. Nicholls, O. Ramström, K. Mosbach, J. Chromatogr. A 691 (1995) 349.
[10] B. Sellergren, M. Lepistö, K. Mosbach, J. Am. Chem. Soc. 110 (1988) 5853.
[11] B. Sellergren, K. Shea, J. Chromatogr. A 654 (1993) 17.
[12] T. Fornstedt, G. Götmar, M. Andersson, G. Guiochon, J. Am. Chem. Soc. 121 (1999) 1164.
[13] C. Baggiani, F. Trotta, G. Giraudi, G. Moraglio, A. Vanni, J. Chromatogr. A 786 (1997) 23.
[14] Y.B. Chen, M. Kele, P. Sajonz, B. Sellergren, G. Guiochon, Anal. Chem. 71 (1999) 928.
[15] G. Guiochon, S.G. Shirazi, A.M. Katti, Fundamentals of Nonlinear and Preparative Liquid Chromatography, Academic Press, Boston, MA, 1994.
[16] M. Jaroniec, R. Madey, Physical Adsorption on Heterogeneous Solids, Elsevier, Amsterdam, The Netherlands, 1988.
[17] G. Götmar, T. Fornstedt, G. Guiochon, Chirality 12 (2000) 558.
[18] T. Fornstedt, P. Sajonz, G. Guiochon, J. Am. Chem. Soc. 119 (1997) 1254.
[19] R.J. Umpleby II, M. Bode, K.D. Shimizu, Analyst 125 (2000) 1261.
[20] I. Quiñones, G. Guiochon, J. Colloid Interf. Sci. 183 (1996) 57.
[21] M. Lepistö, B. Sellergren, J. Org. Chem. 54 (1989) 6010.
[22] S.L. Ajnazarova, V.V. Kafarov, Metodi Optimisatsi Eksperimenta V Khimicheskoy Teknologui, Vishaia Shkola, Moskva, SSSR, 1985.
[23] B. Sellergren, K.J. Shea, J. Chromatogr. A 690 (1995) 29.
[24] E. Bosch, P. Bou, H. Allemann, M. Rosés, Anal. Chem. 68 (1996) 3651.
[25] J. Barbosa, J.L. Beltrán, V.S. Nebot, Anal. Chim. Acta 288 (1994) 271.
[26] T. Mussini, P. Longhi, S. Rondinini, M. Tettamanti, A.K. Covington, Anal. Chim. Acta 174 (1985) 331.
[27] J. Nawrocki, J. Chromatogr. A 779 (1997) 29.
[28] W. Pirkle, J. Chromatogr. 558 (1991) 1.
[29] S. Rybak, B. Jeziorski, K. Szalewicz, J. Chem. Phys. 95 (1991) 6576.